REVIEW OF RESEARCH

IMPACT FACTOR : 5.7631(UIF)

ISSN: 2249-894X

VOLUME - 1 | ISSUE - 1 | MARCH - 2019

THEORETICAL AND EXPERIMENTAL STUDY OF BANDGAP MODIFICATION OF Mg-DOPED ZnS THIN FILMS

Avinash S. Dive[1,*], H. K. Sadekar[2], Ketan P. Gatto[1], Vishnu V. Kutwade[1], M. E. Sonawane[1] and Ramphal Sharma[1]

[1]Thin Film and Nanotechnology Laboratory, Department of Physics, Dr. Babasaheb Ambedkar Marathwada University, Aurangabad

[2]Department of Physics, Arts, Commerce and Science College, Sonai, Ahmednagar, Maharashtra 414105

*Corresponding author: rps.phy@gmail.com

ABSTRACT :

ZnS semiconductor has a wide range of applications in optoelectronics. We present the results of the electronic and optical properties of pure and alkaline earth metal (Mg) doped ZnS by theoretical as well as experimental investigations. The electronic structure is calculated within the full-potential linearized augmented plane wave (FP-LAPW) + local orbitals (lo). The calculated band gap for pure ZnS is 1.53 eV and changes significantly with doping andis found to be1.91 eV.Further,experimentally obtained bandgap for ZnS and Mg-ZnS was found to be 3.51 eV and 3.63 eV respectively. The effect of doping is clearly seen in the optical absorption profiles aswell as in the enhanced electrical conductivities. Due to the widened optical band gap, which suggests higher transmittance in the optical region. There is thepossibility of greater multiple direct and indirect interband transitions due to theavailability of more states compared to pure ZnS.

KEYWORDS : *ZnS, Thin Film, Chemical bath deposition, Optical study, DFT.*

INTRODUCTION

Wurtzite zinc magnesium sulfide(Mg-ZnS) has long been recognized as an important optoelectronic and semiconducting material. In particular, thin films of Mg-ZnS are of great interest due to their efficient application in the fabrication of window layer for solar cells, UV/Visible photodetectors as well as radiation detector[1, 2]. Zinc sulfide (ZnS) is an important II-VI compound semiconductor with a wide direct band gap of ~3.5 eV having higher chemical stability[3].While Mg occurs in the cubic rocksalt structure under ordinary conditions. Theoretically, Mg doping is often used to alloy with ZnS as a common strategy for bandgap engineering and optical confinement[4]. Many reports are available on the successfully prepared $Zn_{1-x}Mg_xS$ alloy with bandgap ranging from 3.5 eV to 4.7 eV[5, 6]. Thus, formed $Zn_{1-x}Mg_xS$ alloy material to be promising in application to ultraviolet band optoelectronic devices[7]. Previously, researcher groups focused on the theoretical as well as experimental investigations of ZnMgS alloys. A. Djelal et. al reported that there is highly misfit in structures of ZnS and Mg due to that some restrictions remain to Mg content $X < 0.35$ % in $Zn_{1-x}Mg_xS$ alloy[8]. Also, other peoples focused on the issue, but they found the onset of the phase segregation starts from $x = 0.35$. Instead of this as per our up to date literature survey there is no report available on the chemical synthesis of $Zn_{1-x}Mg_xS$ alloy and its theoretical correlation. There are many reports available on the physical synthesis technique of ZnMgS such as molecular beam epitaxy[9], pulsed laser deposition, RF sputtering, MOCVD[10], physical vapor deposition etc. But these are costly techniques required expertise to handle the instrument also requires high power and vacuum. Therefore we have chosen the cost-effective single step chemical bath deposition technique.

In this paper, we are reporting a single step, chemical bath deposited $Zn_{1-x}Mg_xS$ thin film and studied their optical and electrical properties using UV-Vis spectroscopic studies as well as I-V characteristics study. The single step chemical bath deposition method is arelativelylow-cost technique which needs low-

temperature treatment as well as low deposition time. To correlates the experimental results we have used the density-functional theory (DFT) calculations, to know the bandgap modification induced by Mg in the ZnS system is investigated.

EXPERIMENTAL DETAILS

The nanocrystalline ZnS and Mg-ZnS thin films were synthesized using the single step, a chemical bath deposition method. The zinc nitrate hexahydrate [$Zn(NO_3)_2.6H_2O$)], magnesium nitrate hexahydrate [$Mg(NO_3)_2.6H_2O$] and thiourea [CH_4N_2S] were used as source materials for the deposition of the ZnS as well as Mg-ZnS thin films. Before deposition, the substrates were cleaned by chromic acid, laboline, deionized water and then air-dried. For the deposition of ZnS thin films 0.5M $Zn(NO_3)_2.6H_2O$ and 0.5M CH_4N_2S were dissolved in 30 ml DI water separately with constant stirring. Three drops of triethanolamine (TEA) were added to the Zn source solution. The pH of the Zn source solution was adjusted to ~11 by dropwise addition of ammonia solution. Further, both the Zn and S precursor solutions were transferred to a beaker. The pre-cleaned glass substrates were immersed vertically in the beaker and the beaker was kept in a water bath at 50 °C for 1 hour. The deposited films were washed with distilled water and dried in air subsequently. The same procedure was followed for the deposition of $Zn_{0.85}Mg_{0.15}S$ thin films, in this case, 0.035M [$Mg(NO_3)_2.6H_2O$] was added as an Mg source to the Zn precursor solution. The synthesized thin films both pure and Mg-doped were found to have a light yellowish color.

The synthesized thin films of ZnS and Mg-ZnS were then characterized for their optoelectronic properties. The electronic transitions in the films were monitored from the optical absorbance spectra recorded in the wavelength range of 300-1100 nm using UV–Vis spectrophotometer Perkin Elmer Lambda-25. The photosensing experiments were recorded by illuminating these nanostructured thin films by different intensities ofthe light source and the data were taken from the computer interfaced with I-V measurement setup KEITHLEY 2400 source meter.

COMPUTATIONAL DETAILS

The band structure and total density of states calculations using first-principles density functional theory (DFT) were performed using the MedeA-(VASP) Vienna ab initio simulation package with the plane-wave pseudopotentials[11]. 2 × 2 × 2 supercellswere built with the wurtzite ZnS unit cell with P63mc as the space group. To study the effect of doping Mg in the ZnS system, two Zinc (Zn) atom was replaced with two Mg atom in the supercell to form ~10 % doping. **Fig.1**(a, b) shows the optimized supercells of ZnS and Mg-ZnS thin films obtained from DFT calculations. The density functional theory calculations were performed using the generalized gradient approximation (GGA) functional with Perdew-Burke- Ernzerhof (PBE) to describe the electron-electron exchange and correlation effect. The DFT equations were solved via projector augmented wave (PAW) method using plane wave basis set as implemented in the Vienna Ab Initio Simulation Package (VASP) interfaced withthe MedeA technology platform. The undoped supercell $(ZnS)_{16}$ consist of 16 Zn atoms and 16 Satoms. Because of two Mg atom in ZnS takes the form as $Mg_2Zn_{14}S_{16}$. The residualforce of 0.01 eV/Å for varying the internal position of atoms was used to attain the minimum energystate as well as 400 eV was set as the cutoff kinetic energy. The 2 × 2 × 2 K-mesh was usedwhich correspond to spacing less than 0.5 Å in reciprocal space. Methfessel-Paxton type ofsmearing was used with a smearing width of 0.2 eV. Real space projection operator was used asthe system contains a large number of atoms.

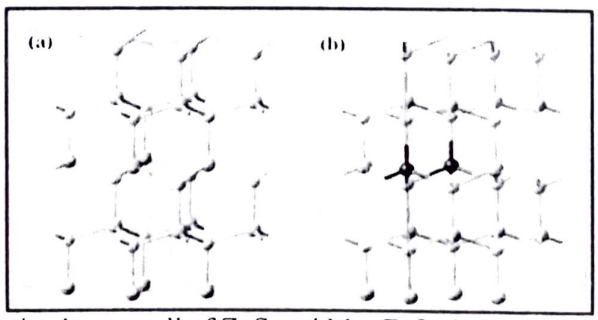

Fig. 1: (a, b) Optimized supercell of ZnS and Mg–ZnS obtained from DFT calculation.

RESULT AND DISCUSSION

Optical study

Fig.2(a),denotes the optical absorbance spectra of the ZnS and Mg-ZnS thin films recorded as a function of wavelength vs. absorbance coefficient. The electronic transitions in the ZnS and the Mg-ZnS thin films can be monitored by studying the absorbance and band gap energy of the materials. The absorbance edges were observed approximately at ~400 nm and ~390 nm for the ZnS and Mg- ZnS thin films respectively[12]. A shift in absorbance edge towards lower wavelength after Mg adding denotes the clear blue shift in energy bandgap which means bandgap increases[13]. The same phenomenon of increase in band gapis also observed in the band structure and density of states (DOS) obtained from DFT[14].The energy band gap was calculated using Tauc's relation equation (1)[15].

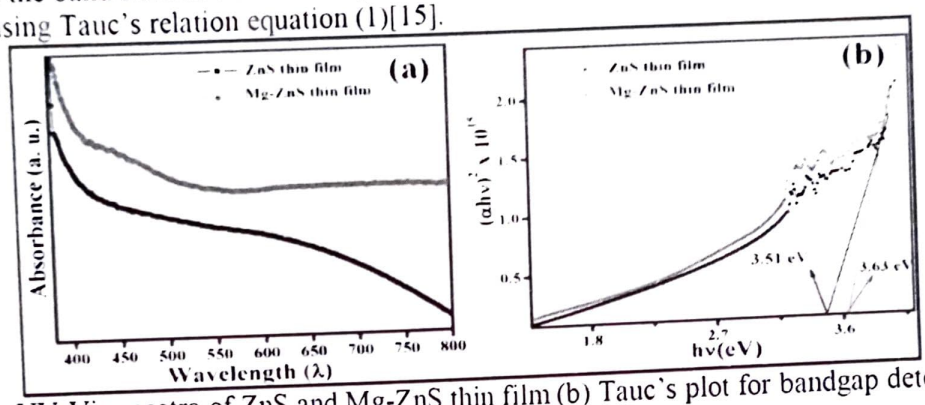

Fig. 2: (a) UV-Vis spectra of ZnS and Mg-ZnS thin film (b) Tauc's plot for bandgap determination.

$$\alpha h\nu = A(h\nu - Eg)^n \quad \ldots\ldots (1)$$

Where α is the absorption coefficient, hυ is the photon energy, A is a band edge sharpness constant and Eg is the energy band gap of the sample. ZnS is a direct bandgap material; the value of n is ½ for the direct transition from valencethe band to the conduction band[11]. The band gap of ZnS and Mg-ZnS is found to be 3.51 eV and 3.63 eV respectively showed in **Fig2**(b).

ELECTRICAL STUDY

The photosensing properties of ZnS and Mg-ZnS thin film were studied by using I-V characteristics in dark and light condition shown in **Fig. 3**(a, b) Silver paste was used to make electrical contacts overthe outlined unit cm^2 active area for the film. The I-Vcharacteristic curve shows linear nature passing through the origin,indicatesthe ohmic nature of the filmshown in **Fig. 3**[11].A strong decrease in resistance after illumination oflight 100W/cm^2 have been observed which is attributed to the generation of freeelectron-hole pairs in the conduction and valence band because of theincident photons[16]. The photon energy breaks the covalent bondswhich increase charge carrier concentration both in the valence bandand conduction band[17].ZnS thin film shows photosensitivity of ~80% and this enhanced after Mg dopingto ~90% estimated using the following equation (2).

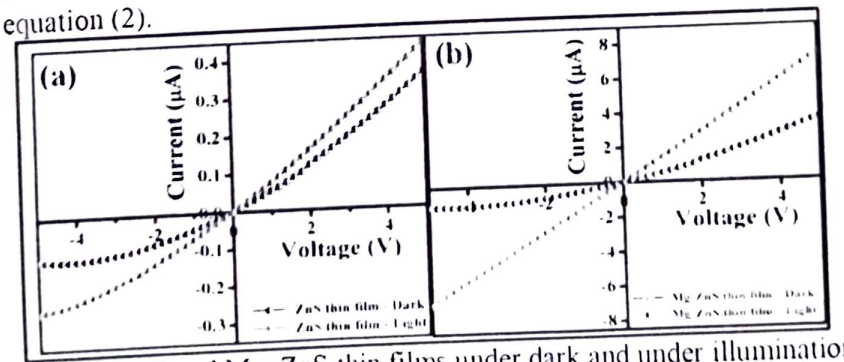

Fig. 3: (a, b) I-V plots of ZnS and Mg–ZnS thin films under dark and under illumination of 100 W/cm^2.

$$S\,(\%) = \frac{R_d - R_l}{R_d} \times 100 \quad \ldots\ldots (2)$$

Where, S (%) Photosensitivity, Rd resistance in dark, Rl Resistance in thelight. Also, we have calculated the change inphotocurrent for ZnS which were found to be 0.20 μA and 5 μA for Mg-ZnS thin

films. Particularly, high sensitivevisible light photoresponse is observed in the Mg-dopedZnS thin film which may be due to some intermediate states made by Mg in ZnS lattice.

ELECTRONIC STRUCTURE INVESTIGATION

In order to confirm the experimental results, theoretical band gap,total, partial and summed density of states have been investigated bythe help of Generalized Gradient Approximation (GGA) of the DensityFunctional Theory (DFT) with the help of Vienna Ab initio SimulationPackage (VASP)[18]. Band structure and minimized supercell geometry of hexagonal ZnS and Mg-ZnS shows in **Fig.4**(a, b). The band gap computed by LDA is which is nearly agrees with our experimental resultsexplained above. In wurtzite phases both the Valance Band (VB) maxima and Conduction Band (CB)minima reside at Γ-point of the Brillouin zone for all considered dopant concentrations showing thatMg-doped ZnS is direct bandgap material. The results obtained by LDA show the increase inband gap when doped by Mg[19].

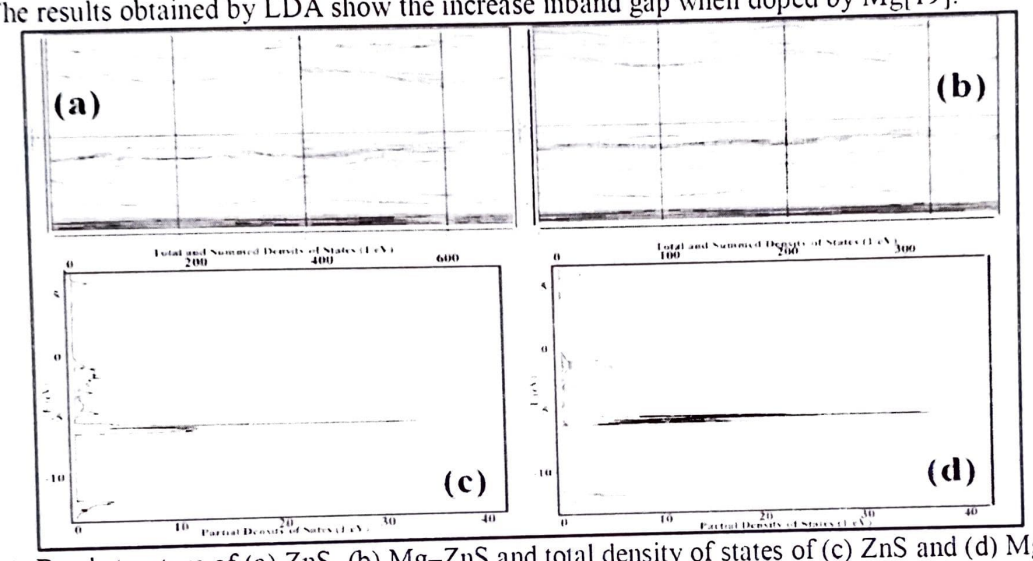

Fig. 4: Band structure of (a) ZnS, (b) Mg–ZnS and total density of states of (c) ZnS and (d) Mg-ZnS.

The character of different energy bands becomes visible in the total and partial Densities of States(DOSs). Total and partial DOS are shown in Fig. The bands belowthe Fermienergy (EF) are Valence Bands (VBs) and above are Conduction Bands (CBS). In **Fig. 4**(c, d) the zeroenergy is taken at the E_F level. The VB can be separated into three parts where the lowest one 'VB1'consists of a mixture of S-3s, Mg-3s, and Zn-4s states whereas peak 'VB2' is due to Zn-3d states and the main 'VB3' is formed by p-states (S 3p). The CB arises from the Zn-4s and Mg-2p orbitals. FromDOS plots shown in **Fig 4**(d)., it is obvious that the band gap has increasedafter Mg doping [20].

CONCLUSION

ZnS and Mg-ZnS thin films were successfully grown by simple chemical bath deposition. The motiveto growth methodis that it is economically cheapest, easy to handle, and low temperature.Asensibleblue-shift in the band gap is achieved forMg-ZnS. UV-Visible spectrophotometry confirms the blue-shift in the bandgap energy of Mg-ZnS ascompared to intrinsic ZnS that can be used in many optoelectronic devices applications. The computational results performed by Medea VASP confirms the blue shift (increasing) bandgapwhich supports the experimentally determined results.

ACKNOWLEDGMENT

Author A. S. Dive is thankful to UGC-DAE CSR Indore for the financial assistance (Ref. No.: CSR-IC-BL-75/CRS-192/2016-17/856). We thanks to Dr. F Singh, scientist IUAC New Delhi, Dr.D. M. Phase, UGC-DAE CSR Indore, for characterization facilities as well as for usefuldiscussion.

REFERENCES

1. Q. L. Huang, L. Fang, H. B. Ruan, B. D. Guo, F. Wu,and C. Y. Kong, Surface Review and Letters 18 (05), 189-195 (2011).
2. X. Si, Y. Liu, W. Lei, J. Xu, W. Du, J. Lin, T. Zhou and L. Zheng, Materials & Design 93, 128-132 (2016).
3. C. Feigl, S. P. Russo and A. S. Barnard, Molecular Simulation 37 (4), 321-333 (2011).
4. G. Kalpana, B. Palanivel, R. M. Thomas and M. Rajagopalan, Physica B: Condensed Matter 222 (1), 223-228 (1996).
5. Z. Charifi, F. E. H. Hassan, H. Baaziz, S. Khosravizadeh, S. J. Hashemifar and H. Akbarzadeh, Journal of Physics: Condensed Matter 17 (44), 7077-7088 (2005).
6. M. Guezlane, H. Baaziz, Z. Charifi, A. Belgacem-Bouzida and Y. Djaballah, Journal of Science: Advanced Materials and Devices 2 (1), 105-114 (2017).
7. I. K. Sou, M. C. W. Wu, T. Sun, K. S. Wong and G. K. L. Wong, JEM 30 (6), 673-676 (2001).
8. A. Djelal, K. Chaibi, N. Tari, K. Zitouni and A. Kadri, Superlattices and Microstructures (2017).
9. I. K. Sou, M. C. W. Wu, T. Sun, K. S. Wong and G. K. L. Wong, Applied Physics Letters 78 (13), 1811-1813 (2001).
10. V. Sallet, A. Lusson, M. Rommeluere and O. Gorochov, Journal of Crystal Growth 220 (3), 209-215 (2000).
11. N. P. Huse, A. S. Dive, K. P. Gattu and R. Sharma, Materials Science in Semiconductor Processing 67, 62-68 (2017).
12. M. M. Fan, K. W. Liu, X. Chen, X. Wang, Z. Z. Zhang, B. H. Li and D. Z. Shen, ACS Appl Mater Interfaces 7 (37), 20600-20606 (2015).
13. I. Khan, I. Ahmad, H. A. R. Aliabad and M. Maqbool, Journal of Applied Physics 112 (7) (2012).
14. M. Dadsetani and A. Zeinivand, International Journal of Modern Physics B 28 (31) (2014).
15. A. S. Dive, N. P. Huse, K. P. Gattu and R. Sharma, AIP Conference Proceedings 1832 (1), 120007 (2017).
16. J. Datta, M. Das, A. Dey, S. Halder, S. Sil and P. P. Ray, Applied Surface Science 420, 566-578 (2017).
17. S. R. Gosavi, C. P. Nikam, A. R. Shelke, A. M. Patil, S. W. Ryu, J. S. Bhat and N. G. Deshpande, Materials Chemistry and Physics 160, 244-250 (2015).
18. I. Djabri, T. Rezkallah and F. Chemam, Chinese Physics B 26 (2), 027102 (2017).
19. Z.-Q. Yu, Z.-M. Xu and X.-H. Wu, Chinese Physics B 23 (10), 107102 (2014).
20. A. Z. M. Dadsetani, International Journal of Modern Physics B 28, 1450211-14502119 (2014).